J|A|C|S
ARTICLES
Published on Web 07/31/2002

Computational Insights on the Challenges for Polymerizing Polar Monomers

Dean M. Philipp,[†] Richard P. Muller,[†] William A. Goddard, III,*[,†] Joey Storer,[‡] Mark McAdon,[‡] and Mike Mullins[§]

Contribution from the Materials and Process Simulation Center (139-74), California Institute of Technology, Pasadena, California 91125, The Dow Chemical Company, Midland, Michigan 48640, and The Dow Chemical Company, Freeport, Texas 77541

Received March 6, 2001. Revised Manuscript Received February 23, 2002

Abstract: Taking Pd di-imine catalysts as an example, we use first principles density functional theory (B3LYP/6-31G*) to investigate the chain propagation steps for polymerization of polar monomers. We start with the complex formed from insertion of ethylene into the polymer chain and consider insertion into the Pd−C bond for each of four polar monomers: methyl acrylate, vinyl acetate, vinyl chloride, and acrylonitrile. We find 2,1-insertion is favored in each case (by 3 to 5 kcal/mol), resulting in a product with a strong interaction of the polar group for the growing polymer chain with the metal. Next, we insert another unit of the same polar monomer or an ethylene unit (except for acrylonitrile). We optimize the structures for all important intermediates and transition states using a continuum dielectric to account for solvation effects. These studies pinpoint the critical difficulties in designing catalysts to polymerize polar monomers.

I. Introduction

In recent years, a great deal of progress has been made in developing commercially important catalysts for olefin polymerization. Much of this progress has involved early transition metals (e.g., Ti and Zr) in Ziegler−Natta type heterogeneous catalysts and in metallocene homogeneous catalysts. These catalysts have proved very valuable and effective for the polymerization of nonpolar olefins such as ethylene and propylene. However, the ability of such catalysts to form high molecular weight homopolymers and copolymers from polar monomers has been very limited, with the main successes involving olefins having polar functional groups very far removed from the vinyl moiety.[1−5] Currently, producing polymers involving such polar monomers is extremely expensive, making it imperative to develop new catalysts that can form homopolymers and copolymers from such fundamental polar monomers as vinyl chloride, acrylonitrile, vinyl acetate, and methyl acrylate. Such catalysts would offer the control of regioselectivity, stereoselectivity, and branching for a growing chain, which all are important in determining the properties of a polymer. In addition, the controlled inclusion of polar monomers in an otherwise nonpolar polymer can provide for vast tailoring of material properties. Consequently, developing catalysts to form homopolymers and copolymers from such polar monomers has been a major quest in polyolefin chemistry.

Boffa et al.[6] recently outlined the progress and strategies for copolymerization of polar monomers with olefins using transition-metal complexes. There remain a number of difficulties that must be resolved before homopolymers and copolymers can be readily made from the fundamental polar monomers. Of special interest is the recent discovery by Brookhart and coworkers of a Pd di-imine catalyst that can form copolymers from ethylene and methyl acrylate, though the incorporation of methyl acrylate is slow and limited to placement at the ends of chain branches.[7] Using this Pd di-imine catalyst as an example, we report herein first principles quantum chemistry calculations [density functional theory (B3LYP/6-31G*)] aimed at delineating the critical challenges associated with forming homopolymers and copolymers from polar monomers. We expect that this will help to focus attention on the changes in the catalysts required to obtain viable high molecular weight polymers and copolymers.

Section II describes the general strategy used in our studies while section III describes the computational methods. The results for ethylene and the four polar monomers are reported and discussed in Section IV. Finally, we summarize the results in Section V.

II. General Strategy

The general strategy we employ to examine the catalytic processes for polar monomers is to use a model system based on the Pd di-imine complex of Brookhart (Figure 1a) to explore

* To whom correspondence should be sent. E-mail: wag@caltech.edu.
[†] California Institute of Technology.
[‡] The Dow Chemical Company, Midland.
[§] The Dow Chemical Company, Freeport.

(1) Chung, T. C. *Macromolecules* **1988**, *21*, 865.
(2) Chung, T. C.; Rhubright, D. *Macromolecules* **1993**, *26*, 3019.
(3) Kesti, M. R.; Coates, G. W.; Waymouth, R. M. *J. Am. Chem. Soc.* **1992**, *114*, 9679.
(4) Aaltonen, P.; Löfgren, B. *Macromolecules* **1995**, *28*, 5353.
(5) Galimberti, M.; Giannini, U.; Albizzati, E.; Caldari, S.; Abis, L. *J. Mol. Catal.* **1995**, *101*, 1.
(6) Boffa, L. S.; Novak, B. M. *Chem. Rev.* **2000**, *100*, 1479.
(7) Mecking, S.; Johnson, L. K.; Wang, L.; Brookhart, M. *J. Am. Chem. Soc.* **1998**, *120*, 888.

10.1021/ja0157705 CCC: $22.00

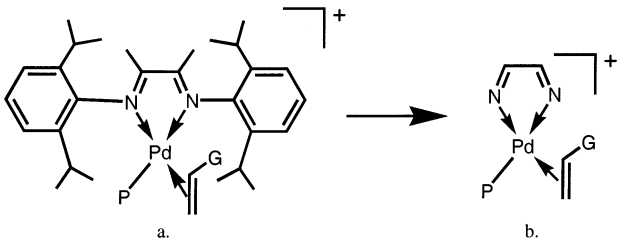

Figure 1. (a) The prototype Brookhart Pd di-imine catalyst. (b) Model system in which hydrogen atoms replace the bulky sidegroups of a. In both structures, P represents the growing polymer and G represents either H or a polar group.

the chain propagation step for polymerization of polar monomers. The Brookhart Pd di-imine catalyst includes bulky 2,6-disubstituted aryl sidegroups that are present primarily to hinder the chain transfer/termination steps in order to obtain high molecular weights. We find that including these groups leads to very small changes in ethylene chain propagation energetics (see Section IVA) and only moderate changes in methyl acrylate propagation (see Section IVB), but dramatically increases the computational expense. Thus, we model the Brookhart type ligand by replacing all sidegroups of the di-imine ligand with hydrogen atoms (see Figure 1b). Of course, inclusion of the bulky sidegroups would be necessary to ascertain energetics for chain transfer/termination steps. We expect that a reasonable understanding of the chain propagation step can be obtained by using just the simple model catalyst in Figure 1b. Also, it will be imperative that inexpensive modeling be sufficient to obtain a qualitatively accurate picture of chain propagation, as such modeling will be used to screen potential catalysts for successful polymerization of polar monomer once the challenges have been ascertained through this current study.

In this study, we initiate chain propagation from the cationic metal complex and optimize the equilibrium structure and transition state structures for the chain propagation step of the catalytic cycle. We seek chain propagation steps without overly stable intermediates since they should favor higher molecular weight polymers (assuming a slow enough rate for chain transfer-termination) and reduce the concentration of dormant or enthalpically trapped active species.

We find that chain propagation proceeds via the Cossée−Arlman mechanism,[8−10] involving a four-center intermediate involving the olefin and metal−carbon bond (for example, see **C** of Figure 4). This mechanism is referred to as a 2s + 2s cycloaddition,[11] and does not involve oxidative-addition. It was originally established for ethylene polymerization by early transition metals (e.g. Ti) but is now supported by recent work on ethylene polymerization by late transition metal catalysts.[12] We model the initial growing polymer chain with an ethyl group, which represents the just-prior insertion of ethylene into the polymer chain. Starting from a metal−ethyl(polymer) complex including a β-agostic hydrogen interaction (Structure **A** in the various figures), the first step is (1) Insertion of a polar monomer (methyl acrylate, vinyl acetate, vinyl chloride, or acrylonitrile), which involves **A** → **B** → **C**→ **D**→ **E** [step a in Figure 2].

For all four polar monomer propagation reactions considered here, we find that 2,1-insertion is favored over 1,2-insertion (by 3.3 to 4.8 kcal/mol). In each case, insertion of the polar monomer leads to a strong interaction with the metal, which challenges subsequent polymerization steps. Except for acrylonitrile, the next step is either (2) insertion of another unit of the same polar monomer [step b in Figure 2] or (3) insertion of an ethylene unit [step c in Figure 2].

For important structures and transition states, we also optimize the structures while including solvation effects (using the Poisson−Boltzmann continuum dielectric approximation as discussed below).

III. Computational Methods

All quantum chemical calculations are carried out using the hybrid B3LYP flavor of density functional theory (DFT) using the Jaguar (v4.0) program.[13] B3LYP includes nonlocal gradient corrections to the Slater local exchange functional[14] and some exact Hartree−Fock exchange. We use parameters[15] referred to as Becke 3 along with the Becke nonlocal gradient correction,[16] the Vosko−Wilk−Nusair exchange functional,[17] and the Lee−Yang−Parr local and nonlocal correlation functional.[18] We solve for the spin-restricted singlet states *without* spatial symmetry constraints. All energies are reported as internal energies (ΔE) without zero point energy, finite temperature enthalpy, or entropy corrections.

The basis set used for Pd is the Hay and Wadt 18-electron relativistic effective-core potential.[19] For all other atoms, the 6-31G* basis set is employed, except for atoms of the di-imine ligand that are not directly coordinated to the Pd atom, for which the 6-31G basis set was used.

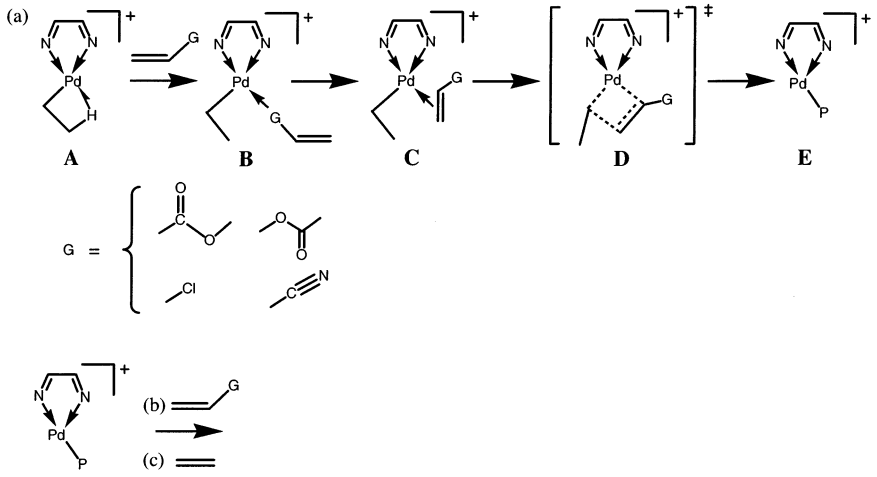

Figure 2. Chain propagation steps. P represents the growing polymer and includes implicit interactions between the polar group and the metal. Reaction a considers the case in which the polar monomer is added to a site at which ethylene was previously added. Reaction b considers the subsequent reactions with a second polar monomer. Reaction c considers the case in which there is a subsequent reaction with ethylene.

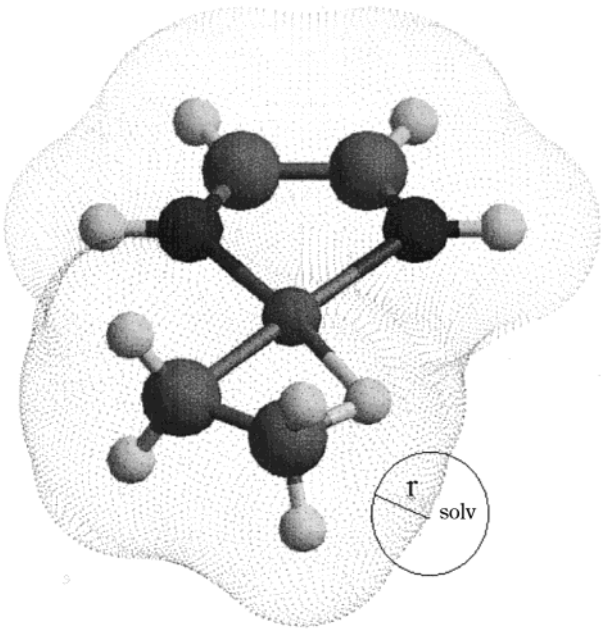

Figure 3. Definition of the solvent accessible surface used in the solvation calculations. Here a solvent sphere is rolled around the van der Waals surface of the molecule and the path of the centroid defines the surface. This is the boundary with the continuum solvent reaction field.

All structures are geometry optimized, corresponding either to minima (zero negative eigenvalues for the Hessian) or transition state structures (one negative Hessian eigenvalue). Transition structure searches are guided by a quadratic synchronous transit method, employing a reactant and a product geometry to aid in the search along a reaction coordinate. Some transition structures presented in the figures are not calculated because they are insignificant numerically (e.g. **E** → **F** in Figure 11, which involves a twist about the Pd−C bond to break the agostic interaction). Others are not calculated because they are virtually barrierless on the vibrationless potential energy surface. Thus for olefin complexation steps (e.g., **A** → **B** in Figure 4), the olefins tend to "float" around with enthalpic barriers that are small or virtually nonexistent,[20] with the rates dominated by entropic contributions. An idea of the entropy involved with monomer complexation can be gained by viewing Table 1. Here, computed values for ΔE, ΔH(298K), ΔS(298K), and ΔG(298K) are given for the respective monomer σ- and π-complexes relative to the starting metal−ethyl complex.

Table 1. Comparison of ΔE, ΔH(298 K), ΔS(298K), and ΔG(298K) for Various Structures Involved in Complexation of Ethylene and Polar Monomers[a]

complex	ΔE, kcal mol^{-1}	ΔH(298K), kcal mol^{-1}	ΔS(298K), cal mol^{-1} K^{-1}	ΔG(298K, kcal mol^{-1}
Pd−ethyl (**A** in all Figs.)	0.0	0.0	0.0	0.0
ETE π-complex (**B** in Figure 4)	−20.2	−17.6	−33.2	−7.7
MA σ-complex (**B** in Figure 6)	−21.9	−19.6	−32.9	−9.8
MA π-complex (**C** in Figure 6)	−20.1	−17.7	−38.2	−6.3
VA σ-complex (**B** in Figure 8)	−17.4	−15.3	−35.2	−4.8
VA π-complex (**C** in Figure 8)	−21.5	−19.3	−44.3	−6.1
VC σ-complex (**B** in Figure 10)	−9.3	−7.2	−32.9	+2.6
VC π-complex (**C** in Figure 10)	−17.4	−15.0	−38.6	−3.5
ACN σ-complex (**B** in Figure 12)	−29.4	−27.0	−30.5	−17.9
ACN π-complex (**C** in Figure 12)	−11.7	−9.4	−35.9	+1.3

[a] All values are relative to the starting metal-ethyl complex. Abbreviations used for the monomers are the following: ETE for ethylene, MA for methyl acrylate, VA for vinyl acetate, VC for vinyl chloride, and ACN for acrylonitrile.

Calculations that include solvation effects use the Poisson−Boltzmann continuum model (PBF)[21−23] available within the Jaguar (v4.0) program. This involves fitting the electrostatic potential of the solvent wave function to a set of atomic charges and solving the Poisson−Boltzmann equation [$\nabla\cdot\epsilon(\mathbf{r})\nabla\phi(\mathbf{r}) = -4\pi\rho(\mathbf{r})$; ϵ is the dielectric, ϕ is the electrostatic potential, and ρ is the charge density, all functions of position **r**] on a mesh using a finite elements approach. Reaction field charges, $\sigma(\mathbf{r})$, are determined at points **r** defining the molecular surface accessible to the solvent, which is determined by rolling a sphere of radius r_{solv} (the probe radius) over the solute surface (see Figure 3). Once the reaction field charges have been found, they are incorporated back into the self-consistent-field (SCF) calculations, and this procedure is done iteratively until convergence is achieved. Jaguar also calculates the forces on the atoms due to the reaction field, allowing the structures to be optimized self-consistently in the polarizing field of the solvent.

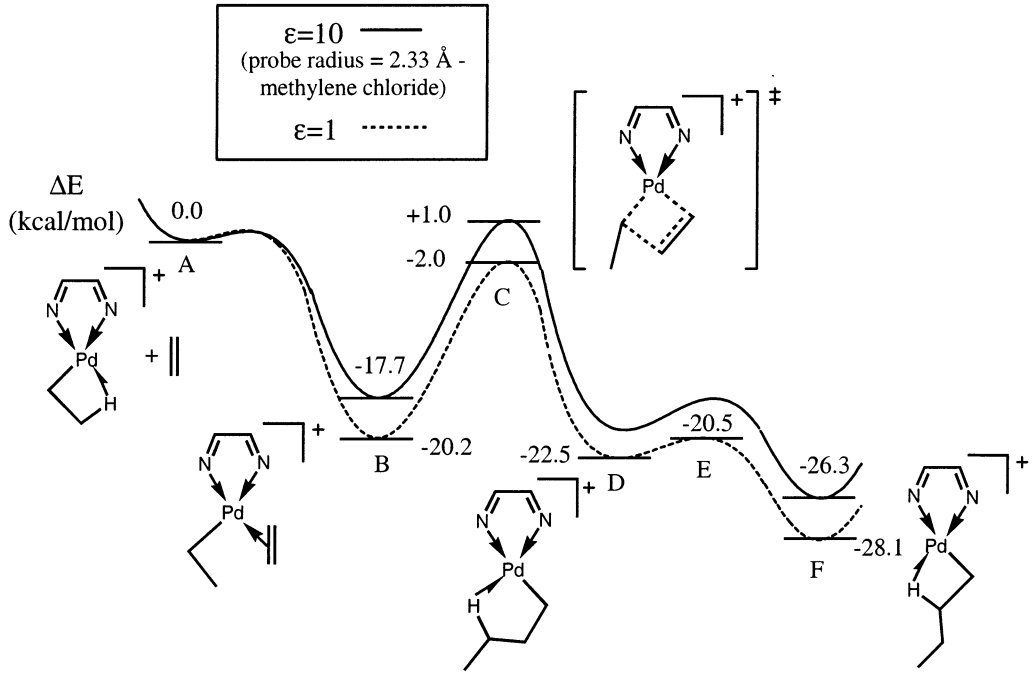

Figure 4. Potential energy diagrams for Pd di-imine catalyst with ethylene. The curves demonstrate insertion of an ethylene unit after a prior insertion of ethylene. The solid curve includes solvation effects while the dotted curve is for the gas phase (vacuum).

In all cases, we use the self-consistent optimum solvated structures, either the local minima (no negative curvatures) or transition state structures (one negative curvature). The resulting solution phase energy is the sum of the solute energy, the polarization energy ($-^1/_2\int_S\sigma(\mathbf{r})\phi(\mathbf{r})d^2\mathbf{r}$), and a cavity term for the energy cost associated with making room for the solute in the solvent.

It should be noted that the continuum solvent model employed in these studies does not involve any explicit solvent molecules. Explicit solvent may be important to determine effects when the solvent directly coordinates with the catalyst (such as would be necessary to accurately determine the entropic effects involved with monomer complexation, as solvent molecules may need to be displaced by the incoming monomer), but a continuum solvent should be adequate for these studies. In addition to the obvious benefit of being much faster and inexpensive, the continuum solvent description has the advantage that thermal averaging over solvent configurations is included implicitly.

Methylene chloride is the solvent used in the Brookhart studies of methyl acrylate/ethylene copolymerization by Pd di-imine catalysts. Consequently, most of our calculations incorporating solvent effects assume parameters appropriate for a methylene chloride solvent (dielectric constant[24] of $\epsilon = 10$ and a probe radius[25] of 2.33 Å). For studies with acrylonitrile monomer, we also consider acetone as a solvent (dielectric constant of $\epsilon = 21$ and a probe radius of $r_{solv} = 2.44$ Å).

We should also note that we do not include the counterions likely to be associated with the charged catalysts considered here. However, the cocatalysts commonly used for α-olefin polymerizations result in large counterions whose structures are sometimes not known experimentally (e.g., MAO/MMAO) and are expensive to model (such as triarylboranes). The fact that our results below show good agreement with experiment, when comparable values are available, justifies our neglect of counterions.

IV. Results and Discussion

A. Ethylene. Potential energy curves obtained for chain propagation of ethylene by the Pd di-imine model catalyst are shown in Figure 4. The dotted curve is for gas-phase results. This can be compared to previous calculations by Morokuma and co-workers[26,27] and by Ziegler and co-workers,[28] which are within a few kilocalories/mole of our results and qualitatively equivalent.

Table 2. Model Ligand System Gas-Phase Comparison of Values for σ-Mode Complexation Energies ($\Delta E_{\sigma-complexation}$), π-mode Complexation Energies ($\Delta E_{\pi-complexation}$), and Barrier to Insertion ($\Delta E^{\ddagger}_{Insertion}$) for the Various Orders of Monomer Insertion Studied[a]

order of monomer insertion	$\Delta E_{\sigma-complexation}$, kcal mol^{-1}	$\Delta E_{\pi-complexation}$, kcal mol^{-1}	$\Delta E^{\ddagger}_{insertion}$, kcal mol^{-1}
ETE-ETE (Figure 4)	-	20.2	18.2
ETE-MA (Figure 7)	23.2	20.6	22.5
MA-MA	0.9	4.9	26.9
MA-ETE	-	5.2	26.6
ETE-VA (Figure 11)	19.2	20.5	16.8
VA-VA	−2.5	−1.9	21.6
VA-ETE	-	3.7	27.2
ETE-VC (Figure 14)	9.3	17.4	18.6
VC-VC	0.8	8.3	24.4
VC-ETE	-	12.6	19.1
ETE-CAN (Figure 16)	29.4	11.7	35.6

[a] Monomer abbreviations are the same as those used in Table 1.

We have also considered the influence of solvation (solid curve in Figure 4), which shows that solvation has only a minor effect on the relative structural energies. Thus, structures **B**, **C**, and **F** are destabilized by 2 to 3 kcal/mol as compared to their nonsolvated counterparts. The resulting barrier to insertion for ethylene is calculated to be 18.7 kcal/mol. This compares well with the experimental value of $\Delta G^{\ddagger} = 17.4$ kcal/mol[7] for ethylene homopolymerization at 25 °C with the substituted Pd di-imine system.

The results in Figure 4 for ethylene propagation serve as a useful benchmark for comparison with the polar monomer studies presented below. All calculated values for complexation energies and insertion energy barriers are tabulated in Table 2 for gas-phase results and in Table 4 for solution-phase results. The complexation energy is the energy difference between the monomer complex (σ-mode or π-mode) and the initial metal−polymer chain (ethyl group or chain with monomer inserted into the ethyl group), and is thus positive when the monomer complex is more stable relative to the metal−polymer chain species. The insertion barriers are defined as the energy difference between the transition structure energy and the energy of the ground state, or lowest energy intermediate.

Figure 5 compares the energetics for gas-phase ethylene polymerization using the full bulky mesityl sidegroups of the complete Brookhart ligand of Figure 1a (solid curve) with the gas-phase results for the model catalyst of Figure 1b (dotted curve), repeated from Figure 4. This confirms that the steric effects of the mesityl groups have little effect on chain propagation. Thus structure **B** in Figure 5 is only 2.9 kcal/mol higher in energy with the mesityl groups included, while structure **C** is 2.6 kcal/mol higher with the bulky groups. Inclusion of solvation with the bulky catalyst results in the bold curve for Figure 5, which is essentially the same as the solid curve for the calculations without solvation (structures **B** and **C** vary in energy by only 0.3 kcal/mol). Thus, solvation does not further influence the results. The complexation energies and insertion barriers are tabulated in Table 3 (gas phase) and Table 5 (solution phase) for this full ligand system.

B. Methyl Acrylate. Because Brookhart and co-workers have successfully made ethylene−methyl acrylate copolymers,[7] we consider first chain propagation of methyl acrylate with the Pd

(8) Cossée, P. *J. Catal.* **1964**, *3*, 80.
(9) Arlman, E. J. *J. Catal.* **1964**, *3*, 89.
(10) Arlman, E. J.; Cossée, P. *J. Catal.* **1964**, *3*, 99.
(11) Steigerwald, M. L.; Goddard, W. A., III *J. Am. Chem. Soc.* **1984**, *106*, 308.
(12) Tempel, D. J.; Johnson, L. K.; Huff, R. L.; White, P. S.; Brookhart, M. *J. Am. Chem. Soc.* **2000**, *122*, 6686.
(13) *Jaguar v4.0*; Schrödinger, Inc.: Portland, OR, 2000.
(14) Slater, J. C. *Quantum Theory of Molecules and Solids, Vol. 4: The Self-Consistent Field for Molecules and Solids*; Mc-Graw-Hill: New York, 1974.
(15) Becke, A. D. *J. Chem. Phys.* **1993**, *98*, 5648.
(16) Becke, A. D. *Phys. Rev. A* **1988**, *38*, 3098.
(17) Vosko, S. H.; Wilk, L.; Nusair, M. *Can. J. Phys.* **1980**, *58*, 1200.
(18) Lee, C. T.; Yang, W. T.; Parr, R. G. *Phys. Rev. B* **1988**, *37*, 785.
(19) Hay, P. J.; Wadt, W. R. *J. Chem. Phys.* **1985**, *82*, 299.
(20) Philipp, D. M. Unpublished result.
(21) Tannor, D. J.; Marten, B.; Murphy, R.; Friesner, R. A.; Sitkoff, D.; Nicholls, A.; Ringnalda, M.; Goddard, W. A.; Honig, B. *J. Am. Chem. Soc.* **1994**, *116*, 11875.
(22) Marten, B.; Kim, K.; Cortis, C.; Friesner, R. A.; Murphy, R. B.; Ringnalda, M. N.; Sitkoff, D.; Honig, B. *J. Phys. Chem.* **1996**, *100*, 11775.
(23) Cortis, C. M.; Friesner, R. A. *J. Comput. Chem.* **1997**, *18*, 1570.
(24) Lide, D. R. *CRC Handbook of Chemistry and Physics*, 74th ed.; CRC Press: Boca Raton, FL, 1993−94. Dielectric constants for 20 °C were used and rounded to the nearest integer.
(25) Probe radius r_{solv} is calculated from $r^3 = 3m\Delta/4\pi\rho$ (10^{24} Å^3/cm^3), where m is the molecular mass obtained by dividing the molecular weight[24] in g/mol by Avogadro's number, Δ is the packing density (assumed to be 0.5 for lack of detailed knowledge of liquid structure), and ρ is the density in g/cm^3 at 20 °C.[24]
(26) Musaev, D. G.; Svensson, M.; Morokuma, K.; Stromberg, S.; Zetterberg, K.; Siegbahn, P. E. M. *Organometallics* **1997**, *16*, 1933.
(27) Musaev, D. G.; Froese, R. D. J.; Svensson, M.; Morokuma, K. *J. Am. Chem. Soc.* **1997**, *119*, 367.
(28) Deng, L. Q.; Margl, P.; Ziegler, T. *J. Am. Chem. Soc.* **1997**, *119*, 1094.

Table 3. Full Ligand System Gas-Phase Comparison of Values for σ-Mode Complexation Energies, π-Mode Complexation Energies, and Barriers to Insertion for the Various Orders of Monomer Insertion Studied[a]

	full ligand system			model ligand system		
order of monomer insertion	$\Delta E_{\sigma-\text{complexation}}$, kcal mol^{-1}	$\Delta E_{\pi-\text{complexation}}$, kcal mol^{-1}	$\Delta E^{\ddagger}_{\text{insertion}}$, kcal mol^{-1}	$\Delta E_{\sigma-\text{complexation}}$, kcal mol^{-1}	$\Delta E_{\pi-\text{complexation}}$, kcal mol^{-1}	$\Delta E^{\ddagger}_{\text{insertion}}$, kcal mol^{-1}
ETE-ETE (Figure 5)		17.2	17.8		20.2	18.2
ETE-MA (Figure 9)	17.2	13.0	20.9	23.2	20.6	22.5

[a] The model system gas-phase results from Table 2 are repeated here for convenient comparison. Abbreviations are the same as those used in Table 2.

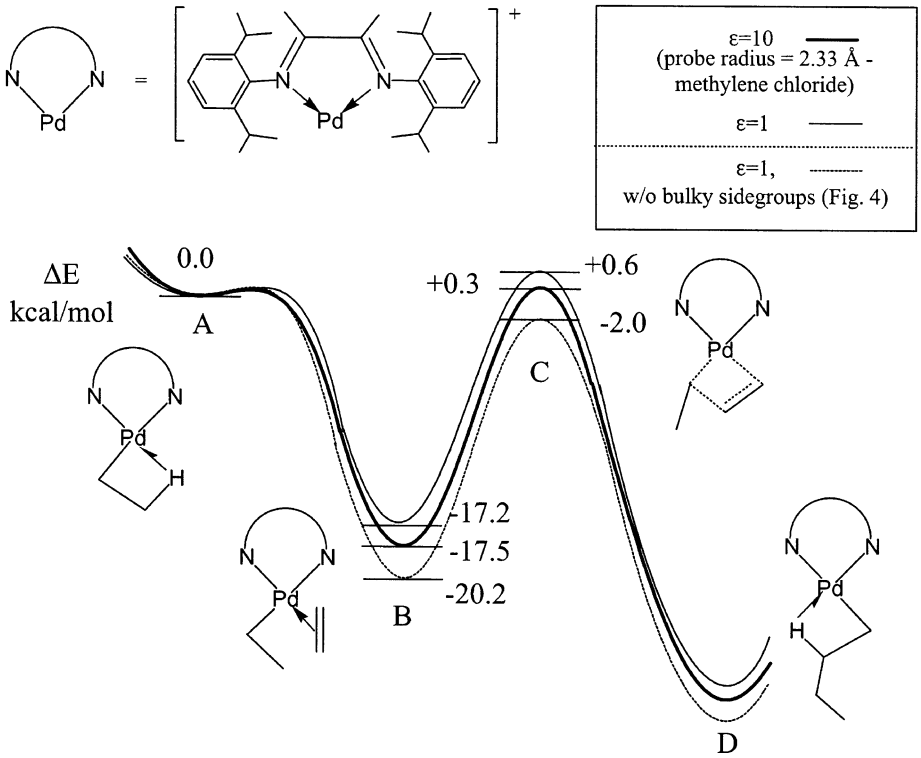

Figure 5. The solid curve (gas phase) and bold curve (including solvation) are the potential energy diagrams for Pd di-imine/ethylene catalyst *including bulky mesityl sidegroups* after a prior insertion of ethylene. The dotted curve reproduces the gas-phase results *without* the bulky sidegroups from Figure 4 (dotted line) for comparison.

Table 4. Model Ligand System Solution-Phase Comparison of Values for σ-Mode Complexation Energies, π-Mode Complexation Energies, and Barriers to Insertion for the Various Orders of Monomer Insertion Studied[a]

order of monomer insertion	$\Delta E_{\sigma-\text{complexation}}$, kcal mol^{-1}	$\Delta E_{\pi-\text{complexation}}$, kcal mol^{-1}	$\Delta E^{\ddagger}_{\text{insertion}}$, kcal mol^{-1}
ETE-ETE (Figure 4)	-	17.7	18.7
ETE-MA (Figure 7)	15.0	13.1	19.2
MA-MA	−3.8	−0.4	22.4
MA-ETE	-	3.0	23.8
ETE-VA (Figure 11)	10.6	14.0	18.7
VA-VA	−7.7	−5.1	27.2
VA-ETE	-	1.9	25.1
ETE-VC (Figure 14)	4.8	13.9	18.6
VC−VC	0.3	9.4	31.6
VC-ETE	-	15.2	26.4
ETE-CAN (Figure 16)	19.3	9.5	25.4

[a] Abbreviations are the same as those used in Table 2.

di-imine model catalyst. The potential energy surface obtained by adding methyl acrylate (after an ethylene insertion) is shown in Figure 6. Figure 7 also includes results showing (a) solvation effects, (b) addition of a second methyl acrylate monomer, and (c) addition of an ethylene monomer after methyl acrylate insertion.

Figure 6 shows that the σ-complex (the O-binding structure **B**) is calculated to be 2.6 kcal/mol more stable than the π-complex (structure **C**). As interconversion between the two should occur readily, the effective transition barrier will depend only on which is most stable. Chain propagation should be prevented from occurring only if one or both of these complexes is overly stable, leading to a prohibitively large barrier to insertion. Methyl acrylate prefers 2,1-insertion over 1,2-insertion by 4.5 kcal/mol (see **D** in Figure 6). After the insertion of methyl acrylate, rearrangements occur easily before subsequent insertions, taking the kinetic product **E** through intermediates **G**, **I**, **L**, **N**, **O**, **Q**, **R**, and **T**. Note that intermediate **G** has a structure in which a lone pair on oxygen donates to the metal, rather than the alternative in which O makes a covalent bond to the metal, with a π-bond between the α- and β-carbons and the metal (**G′** in Figure 8). The product state (structure **U** in Figures 6−8) is predicted to be stable with a strong interaction between the carbonyl oxygen and the metal. Structure **U** is 21.7 kcal/mol lower in energy than the kinetic product **E**! This complexation inhibits any subsequent monomer addition to the catalyst and is consistent with the Brookhart observation that methyl acrylate appears at the end of chain branches. Also, other

Table 5. Full Ligand System Solution-Phase Comparison of Values for σ-Mode Complexation Energies, π-Mode Complexation Energies, and Barriers to Insertion for the Various Orders of Monomer Insertion Studied[a]

	full ligand system			model ligand system		
order of monomer insertion	$\Delta E_{\sigma-\text{complexation}}$, kcal mol^{-1}	$\Delta E_{\pi-\text{complexation}}$, kcal mol^{-1}	$\Delta E^{\ddagger}_{\text{insertion}}$, kcal mol^{-1}	$\Delta E_{\sigma-\text{complexation}}$, kcal mol^{-1}	$\Delta E_{\pi-\text{complexation}}$, kcal mol^{-1}	$\Delta E^{\ddagger}_{\text{insertion}}$, kcal mol^{-1}
ETE-ETE (Figure 5)		17.5	17.8		17.7	18.7
ETE-MA (Figure 9)	13.2	10.8	18.8	15.0	13.1	19.2

[a] The model system solution-phase results from Table 4 are repeated here for convenient comparison. Abbreviations are the same as those used in Table 2.

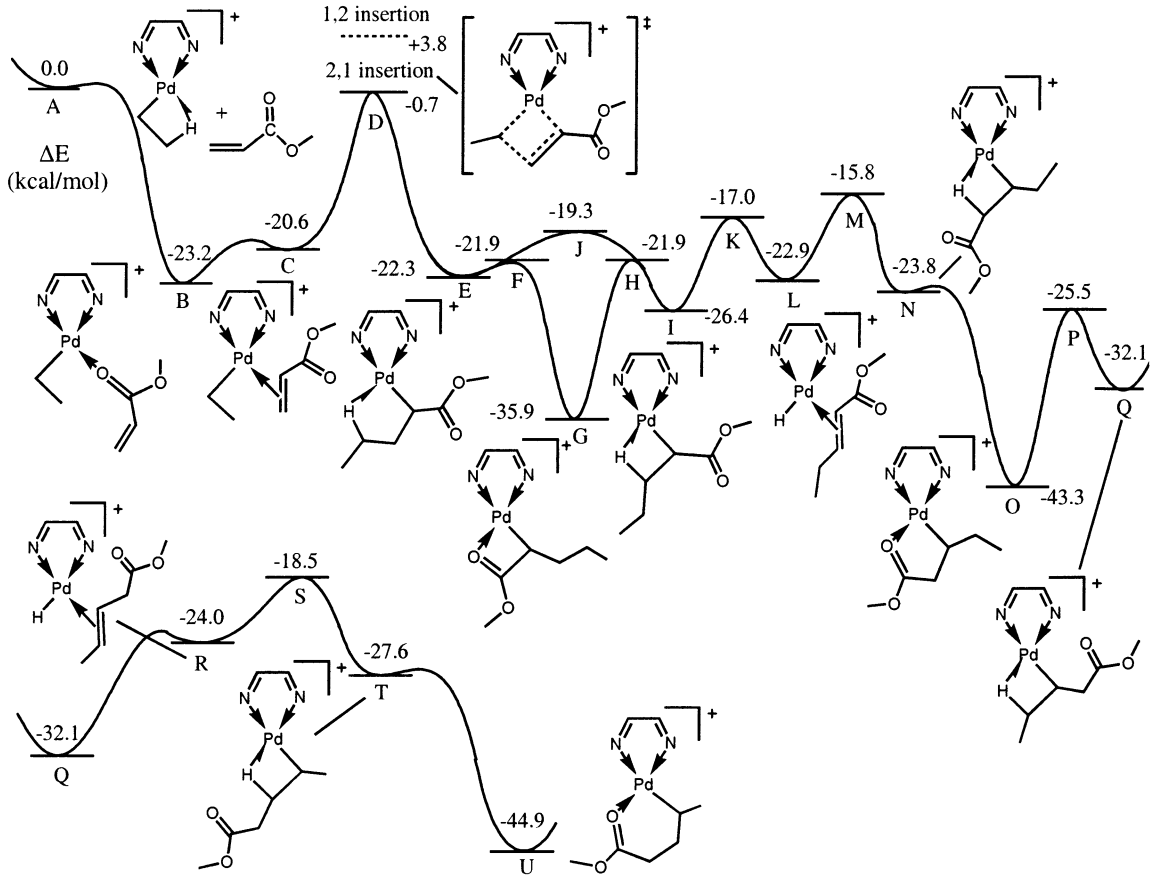

Figure 6. Potential energy diagrams for inserting methyl acrylate into the Pd di-imine catalyst after a prior insertion of ethylene (gas phase).

alternative pathways leading to products with O bonding to the metal are explored in Figure 8, with such products being thermodynamically unfavorable (−5.3 and −6.6 kcal/mol as compared to −44.9 kcal/mol for **U**).

After a methyl acrylate addition, insertion of ethylene (bottom right of Figure 7) has a gas-phase barrier of 21.4 kcal/mol and is preferred over insertion of methyl acrylate, which has a 22.0 kcal/mol barrier. Subsequent insertion of either ethylene or methyl acrylate (bottom left of Figure 7) will be much slower than when preceded by ethylene addition. Gas-phase results are tabulated in Table 2.

We find that solvation does change the relative energies of the various intermediates for chain propagation involving methyl acrylate. However, the overall differences are not extreme and do not change the qualitative conclusions, with the results summarized in Table 4. The calculated barrier to insertion for methyl acrylate into an ethyl group (representing a polymer chain that has just undergone ethylene insertion) is 19.2 kcal/mol. This compares well with the experimental value of $\Delta G^{\ddagger} = 16.3$ kcal/mol at 25 °C (calculated from the reported values of $\Delta H^{\ddagger} = 12.1$ kcal/mol and $\Delta S^{\ddagger} = -14.1$ eu).[7] The relative binding of ethylene vs methyl acrylate is calculated to be 2.7 kcal/mol more stable for ethylene, which is compared to the experimental value of 4.9 kcal/mol.[7] Nonetheless, our results suggest that methyl acrylate insertion should slow polymerization and be limited to the placement at the ends of chain branches, in agreement with the experimental observations of Brookhart.

To address further the issue on the effects of including bulky sidegroups as part of the di-imine ligand, we recalculated the same intermediates and transition states as presented in the top of Figure 7, but with the full ligand of Figure 1a. The results of these calculations are given in Figure 9 and summarized in Table 3 (gas phase) and Table 5 (solution phase), with solid curves showing gas-phase energy surfaces, bold curves solution-phase results, and dotted curves repeating the solution-phase profiles from Figure 7 without the inclusion of the bulky sidegroups. Figure 9 shows that it is at least as important to include solvation effects as it is to include the bulky sidegroups; the important energies are computed to be within a few kilocalories/mole of

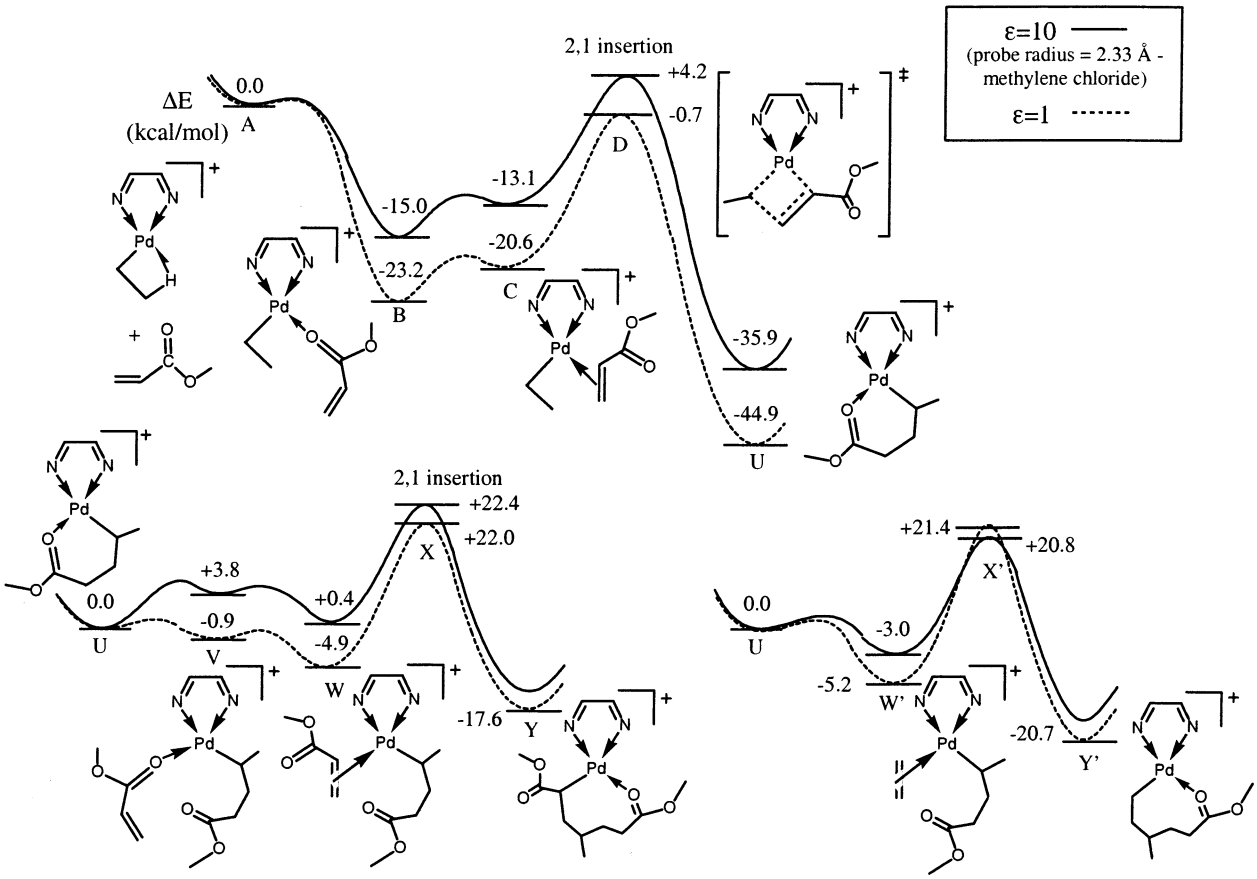

Figure 7. Potential energy diagrams for Pd di-imine catalyst with methyl acrylate *including solvation*. The top curves demonstrate insertion of a methyl acrylate unit after a prior insertion of ethylene. The bottom left curves show subsequent addition of a second methyl acrylate, while the bottom right curves show subsequent addition of ethylene. Solid curves include solvation effects (with a dielectric constant and probe radius representative of methylene chloride solvent), while dotted curves are gas-phase results.

the values for the solution-phase results with the bulky ligand present. Indeed, the dotted curve in Figure 9 does at least as well as the solid curve in approximating the results of the bold curve (results including both the effects of the bulky sidegroups and solvation) for the demonstrated methyl acrylate insertion after ethylene insertion. Of course inclusion of bulky ligands would be necessary to obtain the most accurate representation of the chain propagation involving polar monomers, but this will be necessary only for tuning prospective catalysts once promising catalysts are found that can overcome the difficulties presented here.

C. Vinyl Acetate. After insertion of ethylene, we find the energetics shown in Figure 10 for chain propagation of vinyl acetate monomer. The σ-complex (structure **B**) is less stable than the π-complex (**C**) by 1.3 kcal/mol for vinyl acetate, while 2,1-insertion is again preferred over the 1,2-insertion path, by 3.3 kcal/mol (**D** in Figure 10). After insertion, the very stable complex with the carbonyl oxygen forming a dative bond to the metal (structure **I** in Figures 10 and 11, which is 17.6 kcal/mol more stable than the kinetic product **E**) can be formed after changes in dihedral angles involving low energy barriers. This product is similar to the one formed upon methyl acrylate insertion. As for methyl acrylate, alternative rearrangement pathways leading to products with O bonded to the metal are explored in Figure 12. Again, such products are thermodynamically unfavorable (−10.4 and −32.4 kcal/mol as compared to −46.4 kcal/mol for **I**). Also shown in Figure 12 is the result of chain walking to give a six-membered-ring structure that is found to be less stable (with an energy of −42.7 kcal/mol) than the five-membered-ring structure of **I** (−46.4 kcal/mol).

As with methyl acrylate, vinyl acetate also suffers from a large barrier to subsequent addition of either ethylene or vinyl acetate (see bottom of Figure 11 where the gas-phase insertion barriers are 21.6 kcal/mol for another vinyl acetate and 23.5 kcal/mol for ethylene). These gas-phase results are included in Table 2.

The influence of solvation during vinyl acetate and ethylene copolymerization is revealed in Figure 11. In this case, solvation effects are predicted to be significant, especially for subsequent addition of vinyl acetate monomer, which results in the insertion barrier increasing to 27.2 kcal/mol (25.1 for ethylene). With the inclusion of solvent effects, we observe that subsequent addition of either vinyl acetate or ethylene will experience larger barriers than for the analogous reactions with methyl acrylate, as can be seen in the results summarized in Table 4. Thus, we predict that polymerization involving vinyl acetate will be significantly more difficult than that for methyl acrylate.

D. Vinyl Chloride. Vinyl chloride reaction pathways are given in Figures 13 and 14.

Figure 13 shows the energetics for addition of vinyl chloride after an ethylene insertion. Again 2,1-insertion is favored (by 3.6 kcal/mol; see **D** in Figure 13). Once insertion occurs, rearrangement from structure **E** to structures **F**, **H**, **K**, **M**, and then **O** (similar to the methyl acrylate case) takes place. However, for vinyl chloride we form a β-agostic chloride complex (structure **O** in Figures 13 and 14) that can further

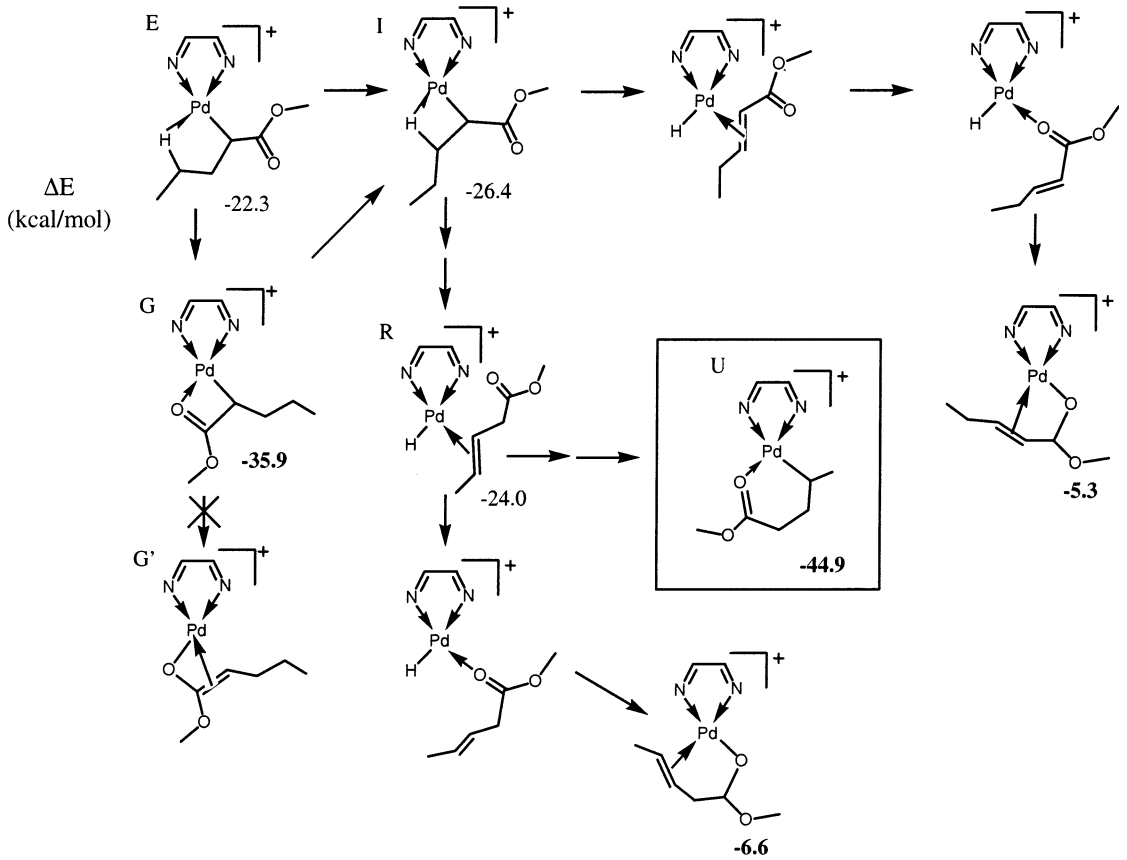

Figure 8. Alternative rearrangement pathways after methyl acrylate insertion. Labeled structures are from Figure 6, with their respective calculated energies.

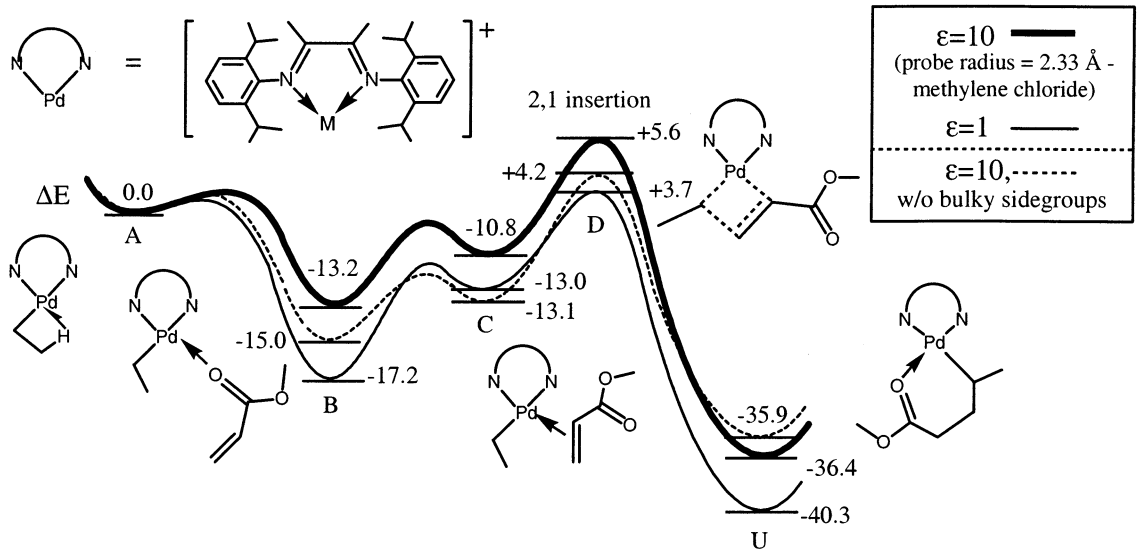

Figure 9. The solid curve (gas phase) and bold curve (including solvation) are the potential energy diagrams for Pd di-imine catalyst *including bulky mesityl sidegroups*. The dotted curve reproduces the solution phase results *without* the bulky sidegroups from Figure 7 (solid line) for comparison. This figure shows methyl acrylate insertion after an ethylene insertion.

react by eliminating chloride to the metal (structure **Q**). Gas-phase results are tabulated in Table 2.

Figure 14 shows the solvation effects. Solvation stabilizes the dissociated chloride species (structure **Q** is now 45.2 kcal/mol more stable than the metal−ethyl complex rather than the gas-phase value of 40.6 kcal/mol), poisoning the active state of the catalyst.

Subsequent addition of either vinyl chloride (bottom left of Figure 14) or ethylene (bottom right) to state **Q** leads to prohibitive barriers (24.4 kcal/mol for vinyl chloride insertion and 19.9 kcal/mol for ethylene insertion; see Figure 14) that become larger when solvation is taken into account (31.6 and 26.4 kcal/mol respectively for vinyl chloride and ethylene insertion). All solution-phase results are included in Table 4.

If another insertion of vinyl chloride could take place, the rearrangement occurring after the previous vinyl chloride insertion would translate into tail-to-tail regioselectivity and polymer branching, two potentially serious disadvantages (this

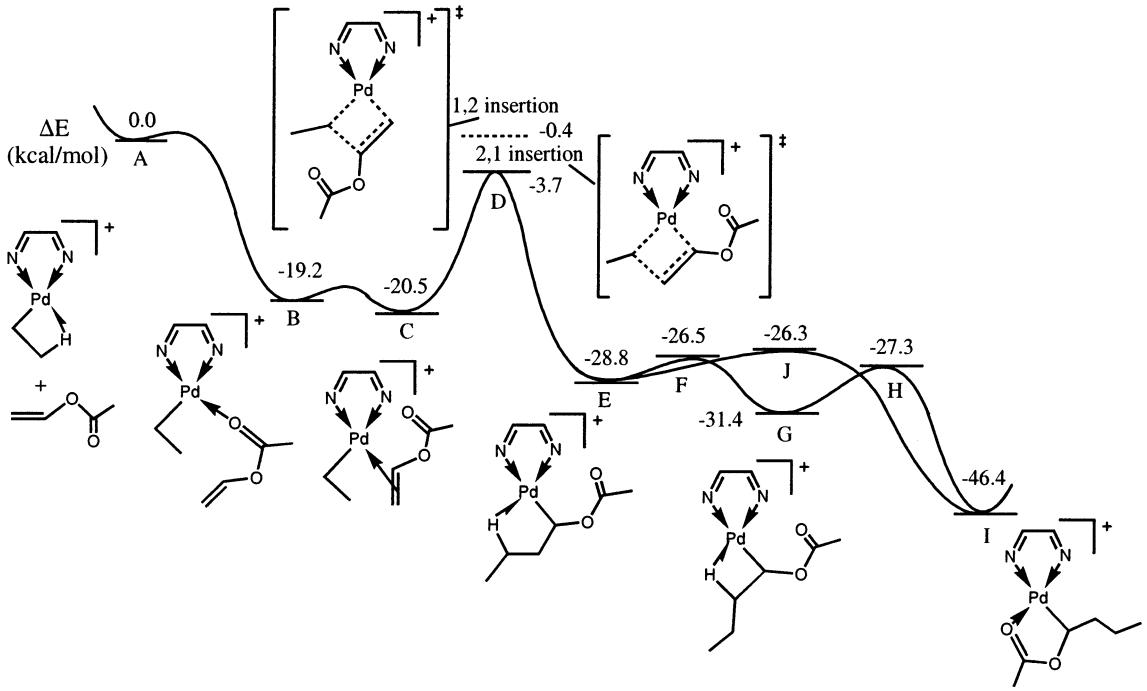

Figure 10. Potential energy diagrams for insertion of a vinyl acetate into the Pd di-imine catalyst after a prior insertion of ethylene.

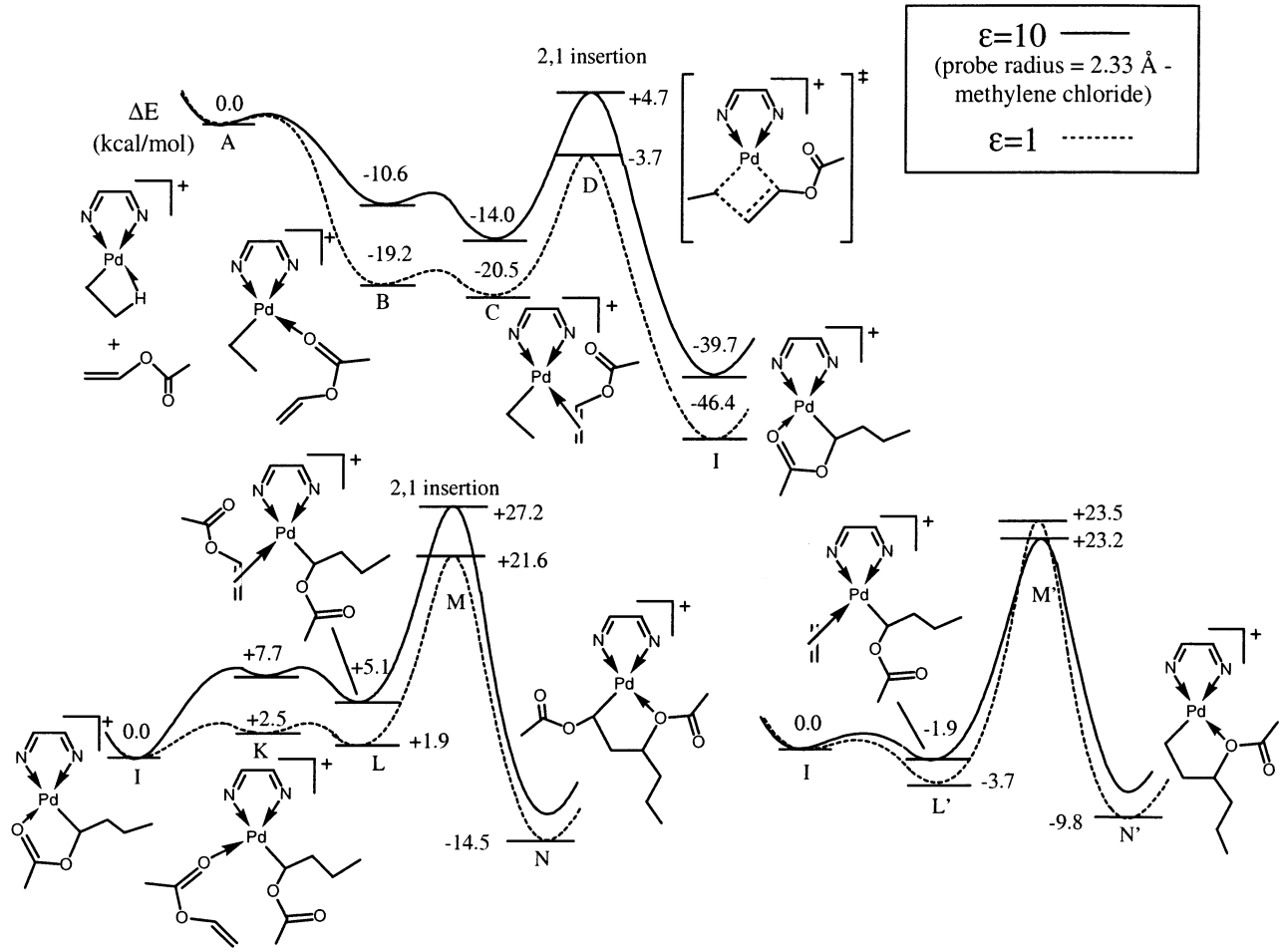

Figure 11. Potential energy diagrams for Pd di-imine catalyst with vinyl acetate *including solvation*. The top curves demonstrate insertion of a vinyl acetate unit after a prior insertion of ethylene. The bottom left curves show subsequent addition of a second vinyl acetate, while the bottom right curves show subsequent addition of ethylene. Solid curves include solvation effects representative of methylene chloride, and dotted curves are gas-phase results.

is similar to what would happen with methyl acrylate). Plus, any control of stereoselectivity could be potentially lost.

E. Acrylonitrile. Chain propagation for acrylonitrile is investigated in Figures 15 and 16.

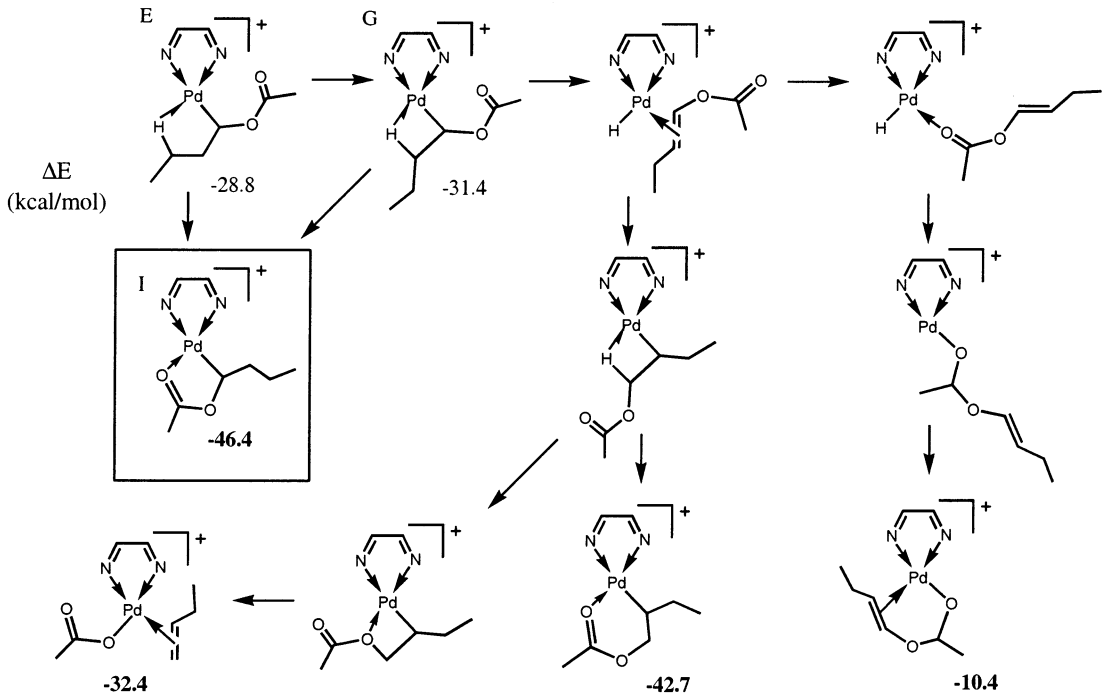

Figure 12. Alternative rearrangement pathways after vinyl acetate insertion. Labeled structures are from Figure 10, with their respective calculated energies.

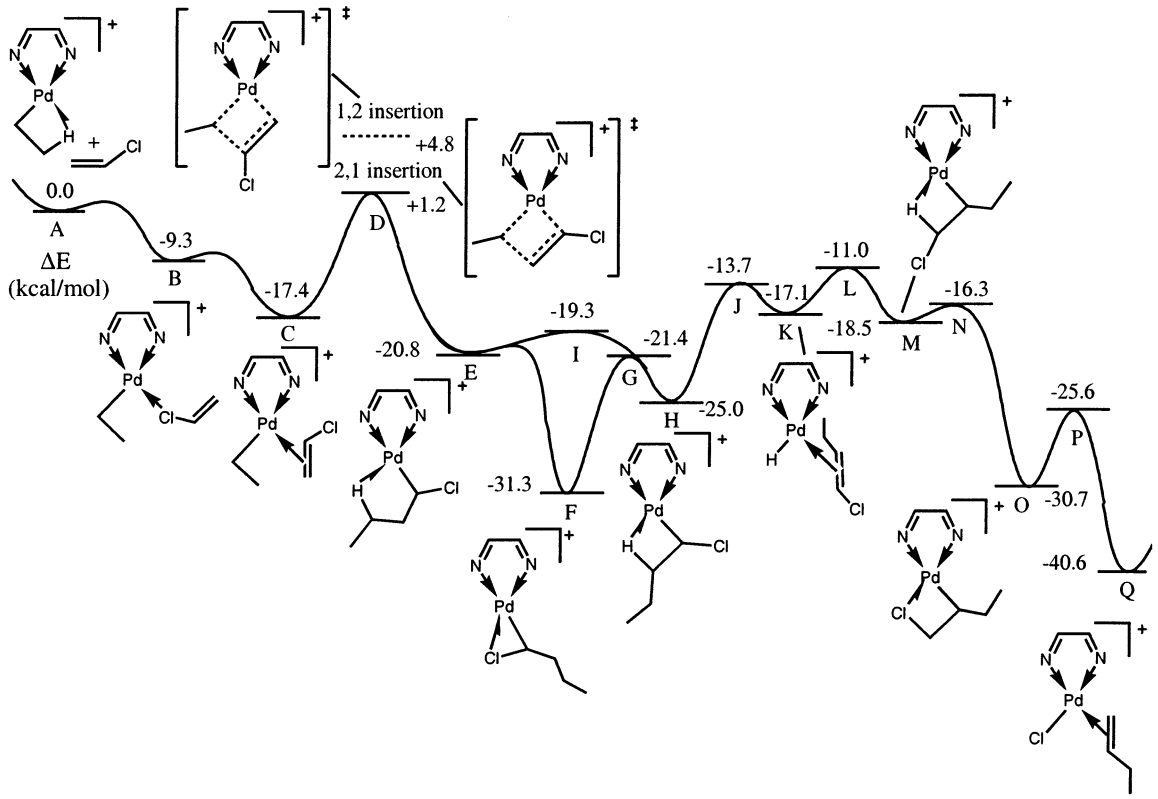

Figure 13. Potential energy diagrams for insertion of a vinyl chloride unit into Pd di-imine catalyst after a prior insertion of ethylene.

The potential energy curve in Figure 15 shows acrylonitrile insertion after an ethylene addition. Like the other polar monomers, acrylonitrile prefers to insert in a 2,1 fashion, with 2,1-insertion being favored over 1,2-insertion by 4.8 kcal/mol in this case. We find that addition is unlikely due to being trapped in a very strong σ-complex, **B** in Figure 15. It would require 35.6 kcal/mol to reach the insertion barrier for transition structure **D**. These findings are consistent with experimental observations that nitriles can inhibit polymerizations.[29]

The curves in Figure 16 illustrate solvation effects, with the results summarized in Table 4 (Table 2 includes the gas-phase values). The results suggest that the σ-complex is destabilized relative to the insertion transition structure (structure **B** is now

(29) Ittel, S. D.; Johnson, L. K.; Brookhart, M. *Chem. Rev.* **2000**, *100*, 1169.

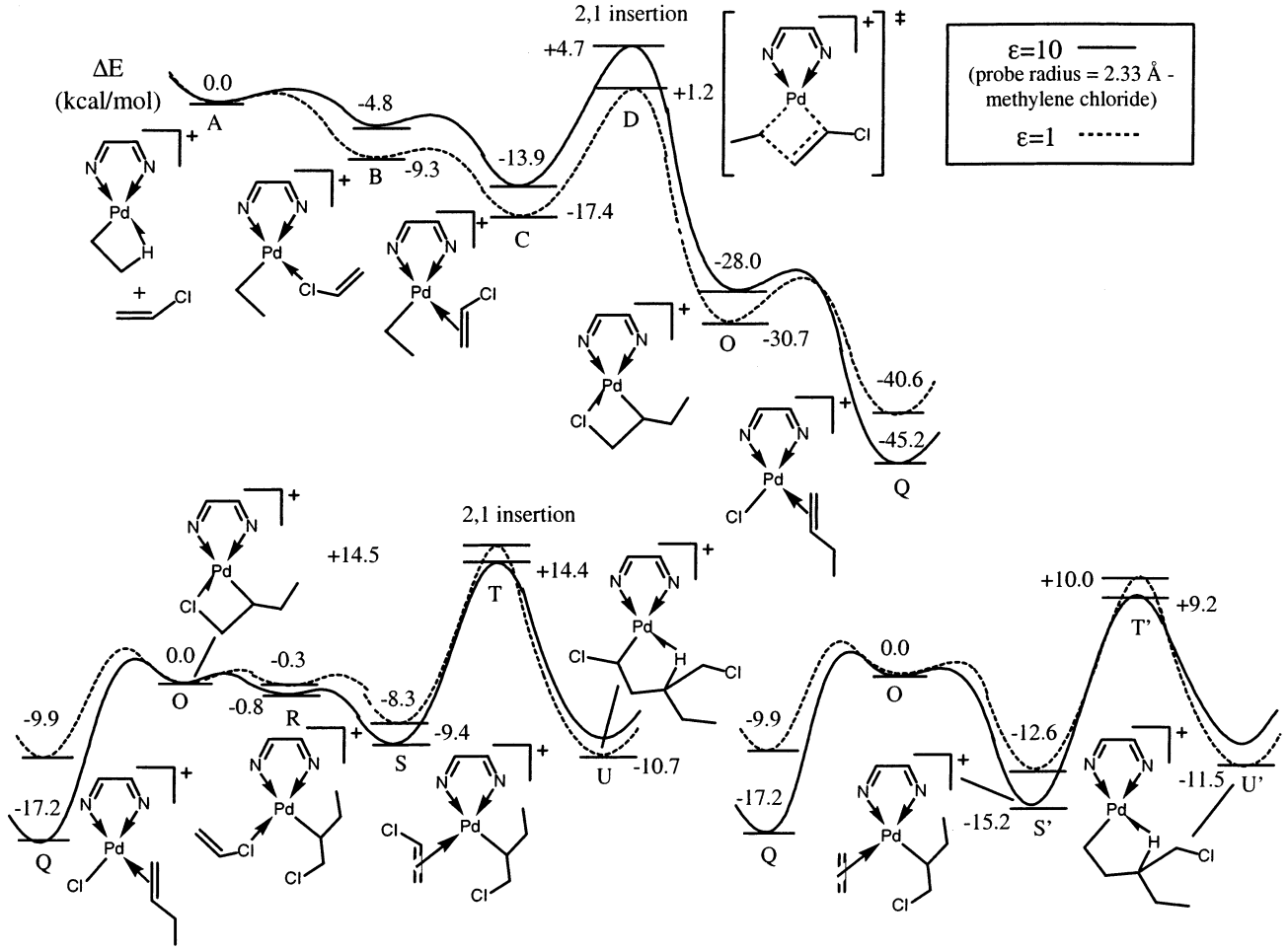

Figure 14. Potential energy diagrams for Pd di-imine catalyst with vinyl chloride *including solvation*. The top curves demonstrate insertion of a vinyl chloride unit after a prior insertion of ethylene. The bottom left curves show subsequent addition of a second vinyl chloride, while the bottom right curves show subsequent addition of ethylene. Solid curves include solvation effects representative of methylene chloride, and dotted curves are gas-phase results.

9.8 kcal/mol more stable than the π-complex **C** and 25.4 kcal/mol below the insertion transition structure **D**). Attempting to further destabilize the σ-complex by increasing solvent polarity to that of acetone[24,25] (dielectric constant $\epsilon = 21$, probe radius = 2.44 Å) yields virtually identical results as for methylene chloride (the solid curve in Figure 16). Since a single insertion of acrylonitrile is highly unfavorable, further insertions of either another acrylonitrile or an ethylene unit were not explored.

F. Discussion. We find that the polar olefins generally form weaker π-complexes with the catalyst than ethylene. This is especially the case for vinyl chloride and acrylonitrile where the gas-phase π-complexation energies from the metal−ethyl complex are respectively 11.7 and 17.4 kcal/mol (as compared to 20.2 kcal/mol for ethylene). Solvation further exacerbates this difficulty as the π-complexation energies from the metal−ethyl complex for methyl acrylate (13.1 kcal/mol), vinyl acetate (14.0 kcal/mol), vinyl chloride (13.9 kcal/mol), and acrylonitrile (9.5 kcal/mol) are all significantly less than the value of 17.7 kcal/mol for ethylene. In addition, all polar monomers will tend to have larger entropy than ethylene (see Table 1), which could definitely play a role in the increased difficulty of forming a polar monomer π-complex. These π-complexes form before monomer insertion occurs, and are then accompanied by higher energy insertion transition states. The transition states energies (kcal/mol) relative to the initial metal−ethyl complex are −0.7 gas-phase (+4.2 solvated) for methyl acrylate, −3.7 gas (+4.7 solvated) for vinyl acetate, +1.2 gas (+4.7 solvated) for vinyl chloride, and +6.2 gas (+6.1 solvated) for acrylonitrile, while ethylene has a transition structural energy of −2.0 gas (+1.0 solvated) relative to the metal−ethyl complex. This leads to larger barriers to insertion for the polar monomers.

Even if it is possible to make an initial insertion, these simulations predict that subsequent additions are prohibitive. Steric effects due to the larger polar olefins may also play a role in limiting propagation rates, especially when the bulky catalyst sidegroups and a longer polymer chain are included.

After submission of this paper, a paper from the Ziegler group appeared[30] that reported similar calculations of binding energies for the Brookhart Pd di-imine catalyst with methyl acrylate and vinyl acetate. They did not report transition barriers or solvation effects, but they did report complexation energies for the π-mode and the σ-mode (referred to by Michalak et al.[30] as an O-complex). For methyl acrylate, they report values for both the model catalyst and the real catalyst that included bulky sidegroups.

Our model system calculations for methyl acrylate (without solvation) give binding energy values of 20.6 and 23.2 kcal/mol for the π-complex and σ-complex (O-complex), while Michalak predicts energies of 20.70 and 17.30 kcal/mol, respectively. For the full catalyst system with mesityl sidegroups,

(30) Michalak, A.; Ziegler, T. *Organometallics* **2001**, *20*, 1521.

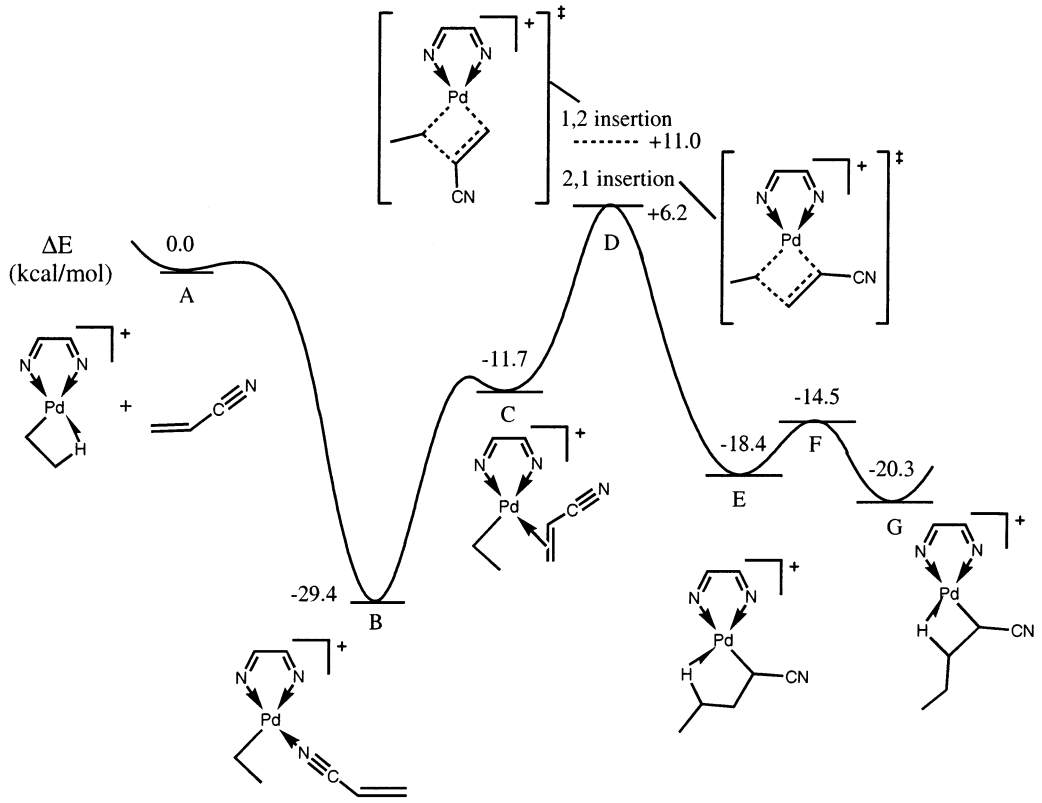

Figure 15. Potential energy diagram for insertion of an acrylonitrile unit into the Pd di-imine catalyst after a prior insertion of ethylene.

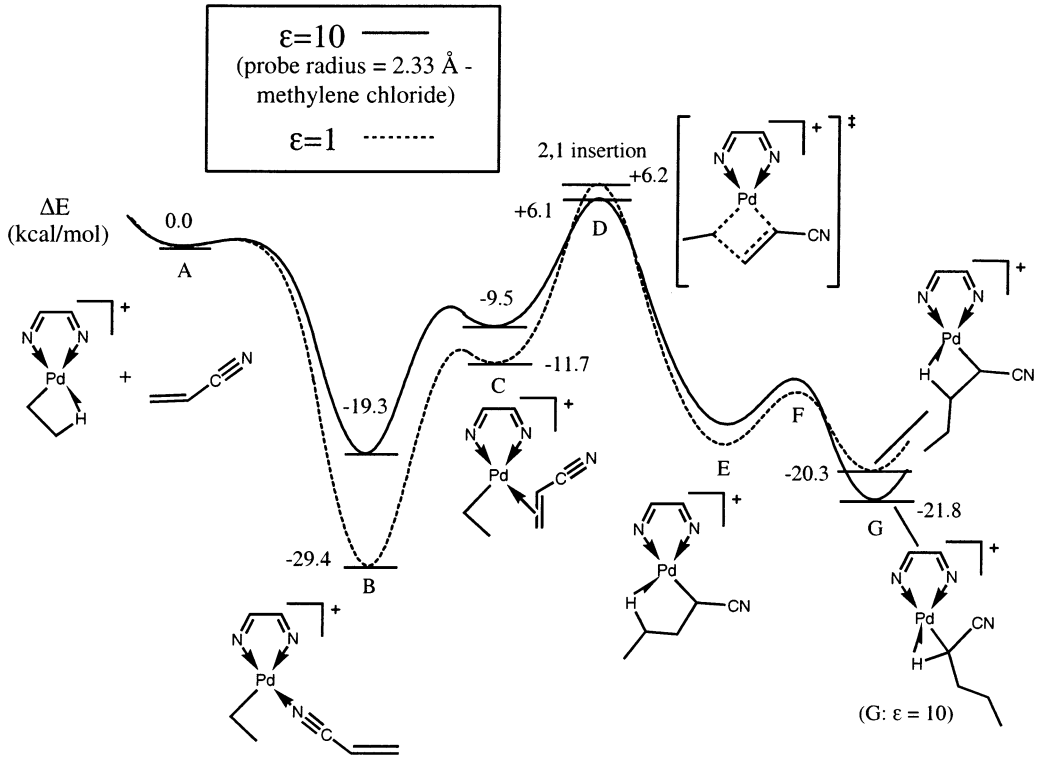

Figure 16. Potential energy diagrams for Pd di-imine catalyst with acrylonitrile *including solvation* after a prior insertion of ethylene. The solid curve includes solvation effects representative of methylene chloride, and the dotted curve is for gas-phase results. The solid curve is virtually the same as for results including conditions representative of acetone ($\epsilon = 21$, probe radius = 2.44 Å).

we obtain gas-phase complexation energies of 13.0 and 17.2 kcal/mol for the π-mode and σ-mode, respectively, while Michalak reports values of 13.65 and 10.64 kcal/mol. Thus for binding in the π-complex, our results and those of Michalak are almost the same, but there is a systematic difference for the σ-complex (O-complex). We find that these differences are mainly attributable to differences in basis sets and to differences in the flavor of DFT used (we use B3LYP while Michalak

BP86). To test the effect of the flavor of DFT, we used BP86 instead of B3LYP to recalculate the energy of the σ-complex, finding it to increase by about 3 kcal/mol. To test the role of basis set we used a triple-ζ basis set rather than double-ζ, where we find an increase by 2 kcal/mol. To test the role of polarization functions on the carboxylate oxygen we removed them, finding an increase by 2 kcal/mol. Thus these effects can account for a difference of 7 kcal/mol in the relative binding energies. Our calculations indicate that including solvation reduces the complexation energies to 13.1 and 15.0 and kcal/mol, respectively, for π- and σ-binding (10.8 and 13.2 kcal/mol with the full ligand system). It is possible to compare these results to experiment. Thus footnote 26 in the Mecking[7] reference states that the O-complex is observed in addition to the π-complex (η^2-olefin complex) at -71 °C but is presumed to be insignificant in typical copolymerization experiments due to rapid rearrangement at room temperature. This suggests that the π-complex is favored energetically by about 1 kcal/mol relative to the σ-complex. This implies that our calculated values for the σ-complex (full ligand) with solvation are about 3.4 kcal/mol too strong, indicating that those of Michalak are too weak by about the same amount.

For vinyl acetate, we calculate gas-phase binding energies of 20.5 and 19.2 kcal/mol respectively for the π-complex and σ-complex, while Michalak computes values of 20.12 and 14.96 kcal/mol, respectively. Again we agree on the π-complexation energies, but disagree by 4 kcal/mol for the σ-complexation energies, probably for the same reasons discussed above for methyl acrylate.

V. Summary

We carried out first principles DFT calculations for chain propagation by a Pd di-imine model catalyst for polymerization of polar monomers. These results indicate that 2,1-insertion of a polar monomer is preferred over 1,2-insertion. In addition we find the following characteristic difficulties in forming polymers from polar monomers:

(a) Methyl acrylate and vinyl acetate insertions lead to products with strong interactions between the carbonyl oxygen and metal. This is consistent with experiments by Brookhart and co-workers, who find that methyl acrylate incorporation is slow and limited to placement at chain branch ends. We find the barriers to subsequent insertions to be even larger after vinyl acetate insertion, predicting that the catalyst would become trapped in this state.

(b) Insertion of vinyl chloride leads to a product in which the chloride prefers to dissociate onto the metal, thus poisoning the catalyst.

(c) Acrylonitrile forms such a strong σ-complex that no further insertions can occur.

(d) Compared to nonpolar olefins, we find that polar olefins often form weaker π-complexes and have larger insertion barriers.

The general major problem with polymerization of polar monomers is that the polar end binds so strongly to the metal (sometimes even dissociating onto the metal) that barriers to subsequent monomer insertions are far too large. Also, rearrangements to further stabilize the intermediate often occur after polar monomer insertion, which will likely increase the difficulties in producing polymers with good regioselectivity and stereoselectivity. It is these challenges that must be overcome in developing new catalysts for homogeneous copolymerization of polar monomers.

Acknowledgment. This work was supported by the Dow Chemical Company. The facilities of the MSC were partly funded by NSF CHE and ARO/DURIP and are also supported by grants from DOE-ASCI, ARO/MURI, Chevron, NIH, ONR, 3M, Seiko-Epson, Avery-Dennison, Kellogg's, General Motors, Beckman Institute, Asahi Chemical, and Nippon Steel.

JA0157705